

## *Supplementary Information*

# **Divergent consensuses on Arctic amplification influence on mid-latitude severe winter weather**

J. Cohen<sup>1,2</sup>, X. Zhang<sup>3</sup>, J. Francis<sup>4</sup>, T. Jung<sup>5,6</sup>, R. Kwok<sup>7</sup>, J. Overland<sup>8</sup>, T. J. Ballinger<sup>9</sup>, U. S. Bhatt<sup>3</sup>, H. W. Chen<sup>10</sup>, D. Coumou<sup>11,12</sup>, S. Feldstein<sup>13</sup>, H. Gu<sup>14</sup>, D. Handorf<sup>5</sup>, G. Henderson<sup>15</sup>, M. Ionita<sup>5</sup>, M. Kretschmer<sup>12</sup>, F. Laliberte<sup>16</sup>, S. Lee<sup>13</sup>, H. W. Linderholm<sup>17,18</sup>, W. Maslowski<sup>19</sup>, Y. Peings<sup>20</sup>, K. Pfeiffer<sup>1</sup>, I. Rigor<sup>21</sup>, T. Semmler<sup>5</sup>, J. Stroeve<sup>22</sup>, P. C. Taylor<sup>23</sup>, S. Vavrus<sup>24</sup>, T. Vihma<sup>25</sup>, S. Wang<sup>14</sup>, M. Wendisch<sup>26</sup>, Y. Wu<sup>27</sup>, J. Yoon<sup>28</sup>

<sup>1</sup>Atmospheric and Environmental Research, Inc. <sup>2</sup>Massachusetts Institute of Technology. <sup>3</sup>University of Alaska Fairbanks. <sup>4</sup>Woods Hole Research Center. <sup>5</sup>Alfred Wegener Institute Helmholtz Centre for Polar and Marine Research. <sup>6</sup>University of Bremen. <sup>7</sup>Jet Propulsion Laboratory. <sup>8</sup>NOAA/PMEL. <sup>9</sup>Department of Geography, Texas State University. <sup>10</sup>Lund University. <sup>11</sup>Potsdam Institute for Climate Impact Research. <sup>12</sup>VU Amsterdam. <sup>13</sup>Pennsylvania State University. <sup>14</sup>Utah Climate Center/Dept. PSC/Utah State Univ. <sup>15</sup>United States Naval Academy. <sup>16</sup>Environment and Climate Change Canada. <sup>17</sup>University of Gothenburg. <sup>18</sup>University of Cambridge. <sup>19</sup>Naval Postgraduate School. <sup>20</sup>University of California, Irvine. <sup>21</sup>University of Washington. <sup>22</sup>University College London. <sup>23</sup>NASA Langley Research Center. <sup>24</sup>University of Wisconsin, Madison. <sup>25</sup>Finnish Meteorological Institute. <sup>26</sup>University of Leipzig. <sup>27</sup>Lamont-Doherty Earth Observatory, Columbia University. <sup>28</sup>Gwangju Institute of Science and Technology.

### **Pattern of Temperature Anomalies**

The Northern Hemisphere (NH) winter temperature anomaly pattern during the era of Arctic amplification (AA) has previously been reported to resemble the pattern of variability associated with the negative phase of the Arctic Oscillation (AO)<sup>1</sup>. Comparison of the winter temperature trends from 1989–2008 with the pattern of variability associated with the negative phase of the AO shows a similar or common pattern (**Supplementary Figure 3a,c**). However, the winter temperature anomalies from 2009–2019 do show a somewhat different pattern with relatively cold temperatures in the interior of the North American and Eurasian continents respectively and

relatively mild temperatures elsewhere. This pattern resembles less the negative AO pattern of variability and possibly more the pattern of variability related to November Barents-Kara Sea ice extent anomalies (**Supplementary Figure 3b,d**). This change in the temperature pattern of variability may or not be a manifestation of the growing influence of sea ice decline on NH winter temperatures in the most recent decade. Also, even though the cooling in Eurasia has received most of the attention<sup>2</sup>, the cold anomalies on the North American continent over the past decade are of comparable magnitude to those in Eurasia.

### **Model vs. Observational Studies**

In an effort to demonstrate the divide in the community and the divide between observational and modeling studies we have created a bar graph listing the number of observational/modeling studies supporting that AA is linked with an increase in severe winter weather and observational/modeling studies supporting that AA is not linked with an increase in severe winter weather (**Supplementary Figure 4**). We estimate that the number of observational and modeling studies are nearly equal, and of course some studies are both. The most lopsided difference is the number of observational studies that support a link between AA and severe winter weather and observational studies that do not. The number of modeling studies that support a link between AA and severe winter weather and modeling studies that do not are more equitably distributed, but we estimate that the number of modeling studies that do not support a link between AA and severe winter weather is greater. In addition, as we show throughout the article, the large ensembles of free-running models including CMIP5, AMIP and the NMME all support that there is no link between AA and increased severe winter weather across the mid-latitudes.

## Arctic Amplification Mechanisms

### Sea Ice

Accelerated Arctic warming has led to, and partly resulted from, a dramatic decline in perennial sea ice cover<sup>3,4</sup>, which has intensified over the last few decades, resulting in a record minimum sea ice extent in September 2007 and a new record in 2012. Seasonally, sea ice decline is most prominent over the western Arctic Ocean in summer and over the Nordic/Barents/Kara Seas in winter. Additionally, the lengthening of the sea ice-free season has been shown to have influenced the interactions between the Arctic atmosphere and surface<sup>5</sup> including increases in surface turbulent fluxes from the ocean to the atmosphere<sup>6</sup>.

Changes in Arctic sea ice during the satellite era have been argued to represent a fundamental change in the Arctic climate system representing a shift from a system dominated by thick, multi-year ice to a “new Arctic” dominated by thinner, first year ice<sup>3,4</sup>. These changes in sea ice cover, as with near-surface air temperature, exhibit a seasonal character marked by the largest changes in fall and winter seasons. However, sea ice decline is also evident throughout summer, unlike Arctic amplification (AA). The character of Arctic climate change provides clues as to the physical mechanisms driving AA including the role of natural variability<sup>7</sup>.

During winter, sea ice decouples the ocean surface from the overlying atmosphere, preventing moderation of Arctic air masses by latent and sensible heat fluxes from the Arctic Ocean. Furthermore, snow accumulations on sea ice mimic the cooling impacts of snow cover over land and hence amplify polar cooling during the long polar night. Given these seasonal roles for Arctic sea ice, even small changes in sea ice cover cause dramatic changes on Arctic climate. For example, anomalously low sea ice during the summer exposes darker (i.e., low albedo) ocean water

to solar radiation, producing strong Arctic warming via absorption of solar radiation in the uppermost ocean layer, and anomalous latent and sensible heat fluxes. This reduction in summer sea ice extent subsequently can affect winter re-growth of Arctic sea ice, allowing for warmer and moister Arctic air masses, particularly over nearby continents. The ensuing feedback leads to amplified warming of the Arctic relative to the rest of the globe<sup>8,9</sup>.

## **Clouds**

Arctic clouds warm the surface via enhanced downwelling longwave radiation for much of the year, except during the summer months when the shortwave cloud radiative effect dominates, cooling the surface<sup>10</sup>. Due to the significant cloud radiative effects, changes in cloud amount or optical properties constitute a potentially important and uncertain feedback on AA. For instance, results from the Fifth Coupled Model Intercomparison Project (CMIP5) climate models disagree about whether Arctic cloud changes dampen or amplify AA<sup>11</sup>. A potentially important process contributing to Arctic cloud feedback is the cloud response to Arctic sea ice declines in response to increased surface turbulent heat and moisture fluxes. Recent observational evidence points to a significant cloud response to sea ice decline in fall, constituting a positive feedback that increases downwelling longwave radiation supporting a delayed sea ice freeze onset<sup>10</sup>. In contrast, in summer there is no significant cloud response, which would enhance reflected shortwave radiation and be a negative feedback on Arctic warming. Overall, state-of-the-art CMIP5 climate models point to a small positive cloud contribution to AA, primarily in fall and winter<sup>6</sup>.

## **Longwave Radiation**

Downward longwave radiation has also been identified as an important contributor to AA<sup>12,13,14</sup>. Emerging evidence suggests that anomalous cloud cover and downward longwave radiation during winter can hinder sea ice growth, thus reducing Arctic sea ice cover the following summer<sup>15,16,17</sup>. The CMIP5 climate models indicate that changes in the downwelling clear-sky longwave flux from the atmosphere, rather than the surface albedo feedback, is the largest contributing factor to AA<sup>11</sup>. The downward longwave radiation trend is positive almost everywhere over the Arctic Ocean for all seasons (see Figure 3 from Cohen et al.<sup>18</sup>). Warm, moist air intrusion events and attendant cloud radiative forcing have been found to regularly occur in Arctic winter<sup>19,20</sup> and generate significant downwelling longwave radiation anomalies at the surface<sup>21</sup>. And similar extreme moisture transport into the Arctic in spring has been found to play an important role in determining the minimum sea-ice extent in the following September<sup>22,23,24</sup>. Moisture transport is most pronounced through the North Atlantic pathway and is favored during blocking events in the Atlantic sector<sup>23</sup>.

## **Tropical Convection**

Tropical convection may also play an important role in forcing AA via heat and moisture transports during the cold season when the strong subtropical jet is conducive for a convection-driven Rossby wave propagation. Tropical convection can excite moisture intrusion events and Arctic warming on inter-decadal time scales<sup>25,26,27</sup>. Furthermore, intraseasonal tropical convection also appears to influence daily Arctic surface temperature and sea ice concentration via the Madden-Julian Oscillation phase 5 in both summer and winter<sup>28,29,30</sup>. These heat and moisture transports are

enhanced by poleward propagating Rossby waves, excited by the tropical convection, that constructively interfere with the climatological stationary eddies<sup>16,26,31</sup>.

## **Regional Response of AA**

### **Asia**

Over the past decade, there is increasing evidence of a dynamical pathway, beginning with negative sea ice and positive air temperature anomalies over the Barents-Kara Seas during autumn, linking to cold Central and Far East Asia temperatures in mid-to-late winter<sup>32,33</sup>.

In December and January, the additional oceanic heat and moisture release from newly open waters in the Arctic Ocean to the atmosphere can increase Siberian snow cover<sup>34</sup>. The increased snow cover may enhance continental cooling and troughing over East Asia while strengthening the Siberian high upstream over northwest Eurasia<sup>35</sup>. The anticyclonic anomaly is often centered over the Barents-Kara Seas and Ural regions, bringing cold air from the Arctic to central Asia, which extends southeastward owing to a strengthened Siberian High. This southward flow of Arctic air has been implicated in more frequent or intensified cold surges over East Asia in recent decades<sup>36,37</sup>.

### **North America**

Potential connections between the North American Arctic and mid-latitude weather depend on the constructive or destructive interactions with locations of existing large-scale waves in the jet stream. Climatological waves during winter usually consist of a block or ridge of higher

geopotential heights over the northeastern Pacific and Alaska and/or Greenland along with a trough of lower heights over central and eastern North America, although a great deal of interannual variability is common<sup>38</sup>. Of particular interest is the observed winter cooling trend in eastern North America since 1990<sup>1</sup>. Although this trend coincides with Arctic warming<sup>39,40,41</sup>, studies have also pointed to internal variability<sup>42</sup> and influences from the tropical Pacific<sup>43,44</sup>. More recent work suggests a tropical response to Arctic warming that feeds back to the Arctic<sup>26</sup>.

The potential for the Arctic to influence eastern North America involves a modification and added persistence to the existing long-wave pattern. Higher regional Arctic geopotential heights increase the likelihood of Alaskan and/or Greenland blocks; further analyses suggest that these regional blocks are independent features<sup>42,45,46</sup>. The geopotential height ridge along the west coast of North America along with low heights over eastern North America are an amplification of the climatological late-autumn/early-winter wave pattern. The anomaly pattern over the North Atlantic Ocean exhibits a strong downstream storm track coincident with eastern North America cold events. While these historical teleconnections do not necessarily involve Arctic change<sup>39</sup>, recent temperature trends (1988/89–2014/15) suggest a winter connection between warm temperatures in the Chukchi Sea and cold spells in eastern North America. Similarly, recent studies found that regional positive sea surface temperature anomalies were linked to Greenland blocks and years of extreme late freeze conditions in Baffin Bay since 2006<sup>45,46</sup>.

## **Europe**

Variability in Europe's weather is principally associated with the North Atlantic Oscillation (NAO) and high-pressure cold air masses from the east. During negative NAO episodes, Greenland blocking tends to be associated with a southward displaced storm track across the eastern Atlantic,

which favors cold winters in northwestern Europe<sup>47</sup>. Reduced sea ice in the Baffin Bay, Davis Strait and the Labrador Sea is related to stronger Greenland blocking, an equatorward shifted Jet Stream and colder temperatures across Northern Europe<sup>46</sup>. In addition, evidence of connectivity between Barents-Kara sea ice loss and winter weather in northern Europe has been reported<sup>33,48,49</sup>. Modeling experiments show a diversity of NAO responses to reduced Arctic sea ice. The atmospheric response is dependent on the sign<sup>49</sup>, the pattern<sup>50,14</sup> and the amplitude<sup>48,51,52,53</sup> of the sea ice anomalies.

## **Summer**

While linkages in early winter have received the most attention by researchers owing to their influence on extreme winter weather, progress has also been made in understanding summer linkages. Here, there is an interaction of newly open water areas, atmospheric and oceanic frontal features, and phasing with high-amplitude/high-wavenumber atmospheric circulation features<sup>54,55</sup>. In addition, the loss of snow cover favors earlier and more intense heating of the land areas surrounding the Arctic ocean. This is consistent with the pattern of AA during summer as the regions of largest positive 1000-500 hPa thickness anomalies occur mainly over land. This earlier onset of continental warming has been linked to more frequent extreme heat waves and persistent summer weather patterns<sup>55,56</sup>.

The summer season has seen an overall weakening of storm tracks over the last decades<sup>56</sup> and this is also projected by model simulations of future climate change<sup>57,58</sup>. How a weakened flow might affect weather systems, their frequency and persistence, is not fully understood<sup>59</sup>. See Coumou et al.<sup>60</sup> for a more in-depth review of summer linkages.



## Summer vs. Winter Forecasts

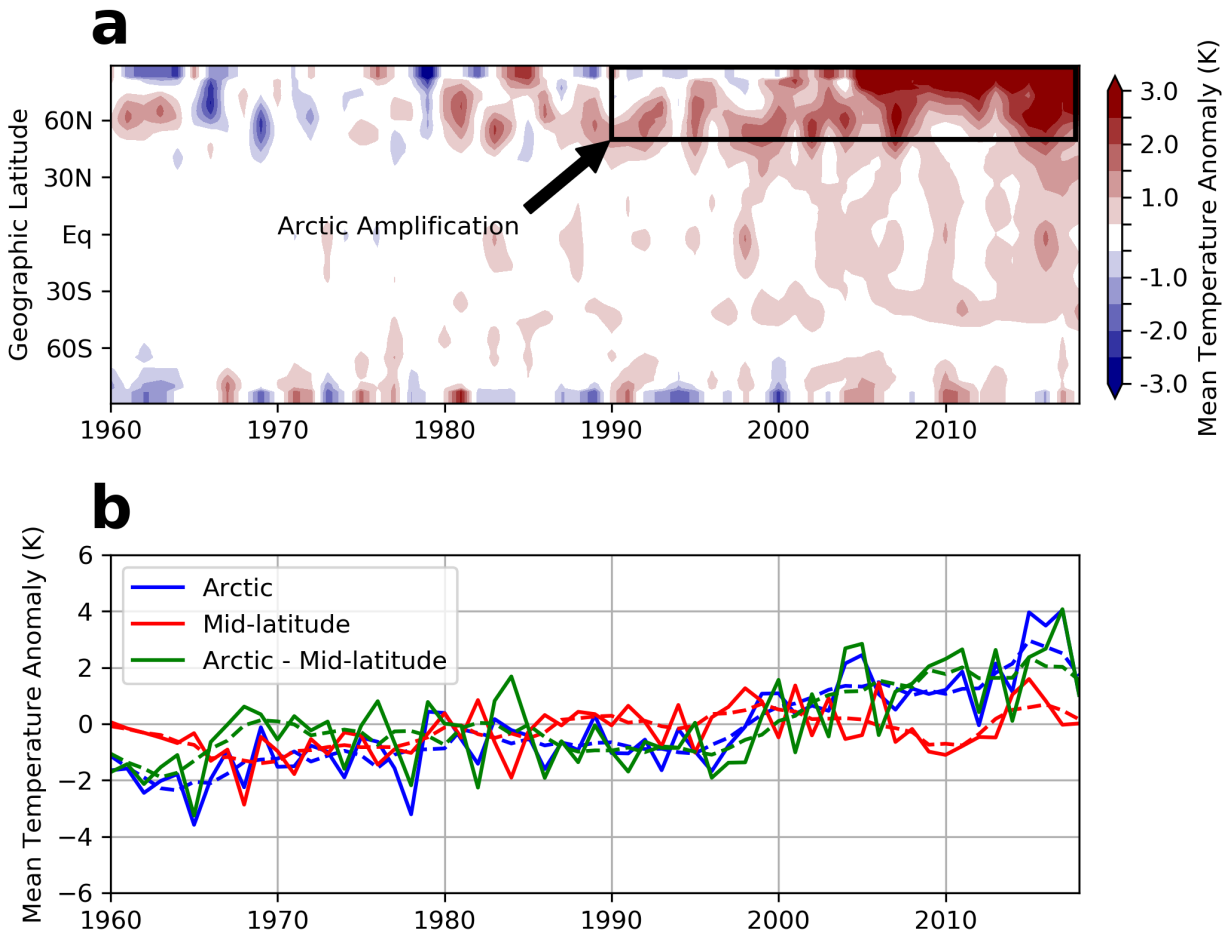
As seen in **Figure 4** the NMME winter temperature forecasts are diverging to the warm side from the observed winter temperatures across the mid-latitude continents. In **Supplementary Figure 11** we present the analogous of **Figure 4** but for summer. In contrast to winter, the NMME summer temperature trend is nearly parallel to the observed summer trend across the mid-latitude continents despite the cold bias. It is pertinent to our understanding of AA mid-latitude linkages as to why the model simulated temperature trends diverge from the observations across the mid-latitude continents in winter but not in summer.

A rare observational analysis outlier argued that AA does not force colder winter temperatures across the mid-latitude continents<sup>61</sup>. The authors, based on turbulent heat fluxes (sensible plus latent heat flux or THF), differentiated between winter seasons when the Arctic ocean forced the atmosphere and when the atmosphere forced the Arctic ocean. Those winters when sea ice was low (high) and the anomalous THF is upward (downward) then the Arctic ocean is forcing the atmosphere and when sea ice was low (high) and the anomalous THF is downward (upward) then the atmosphere is forcing the Arctic ocean. They then showed that the warm Arctic/cold continent (WACC) pattern only exists when the atmosphere is forcing the Arctic Ocean but when the Arctic Ocean is forcing the atmosphere, the Arctic is warm but the continents are no longer cold.

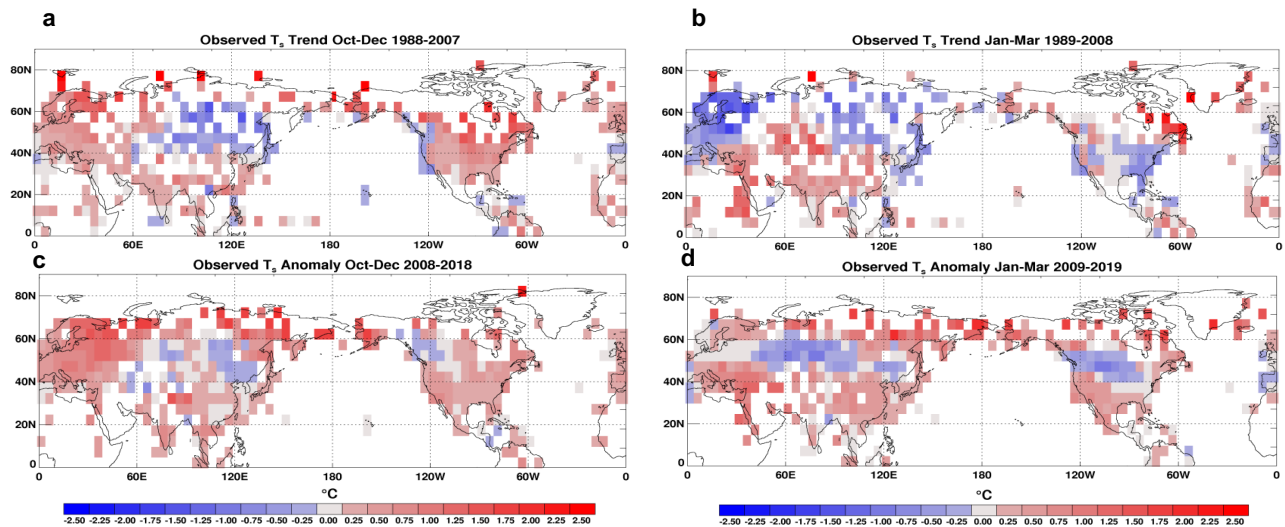
Whether the winters were divided into atmosphere forcing the ocean or vice versa the net THF anomaly was always negative or downward, which indicates a net heating of the ocean but a net cooling of the atmosphere. Therefore, that the atmosphere was relatively warm in all cases, likely indicates that the analysis is not in energy balance, especially for those winters where the ocean forces the atmosphere since the anomalies were an order of magnitude larger than when the atmosphere forces the ocean.

A cleaner comparison is to take the difference between summer and winter. In winter the absolute THF value is positive or upward and the difference between THF in summer and winter is negative or downward (as well as the difference in the trends) especially over open water<sup>6</sup>. In **Supplementary Figure 12a** we show the differences in temperature trends between summer and winter, where the THF are negative in the absolute sense and represents the atmosphere forcing the ocean. For summer minus winter the differences in the temperature trends during the period of AA or strong sea ice melt, the Arctic is relatively cold, and the mid-latitudes are relatively warm. In **Supplementary Figure 12b** we show the differences in temperature trends between winter and summer, where the THF are positive in the absolute sense and represents the ocean forcing the atmosphere. For winter minus summer, the Arctic is relatively warm, and the mid-latitudes are relatively cold. Importantly in this analysis, the Arctic temperatures are consistent with the sign of the THF difference, indicating that the analysis is in energy balance. Based on the THF summer and winter difference only, the warm Arctic and cold continents pattern only exists for when the Arctic ocean is forcing the atmosphere and not vice versa.

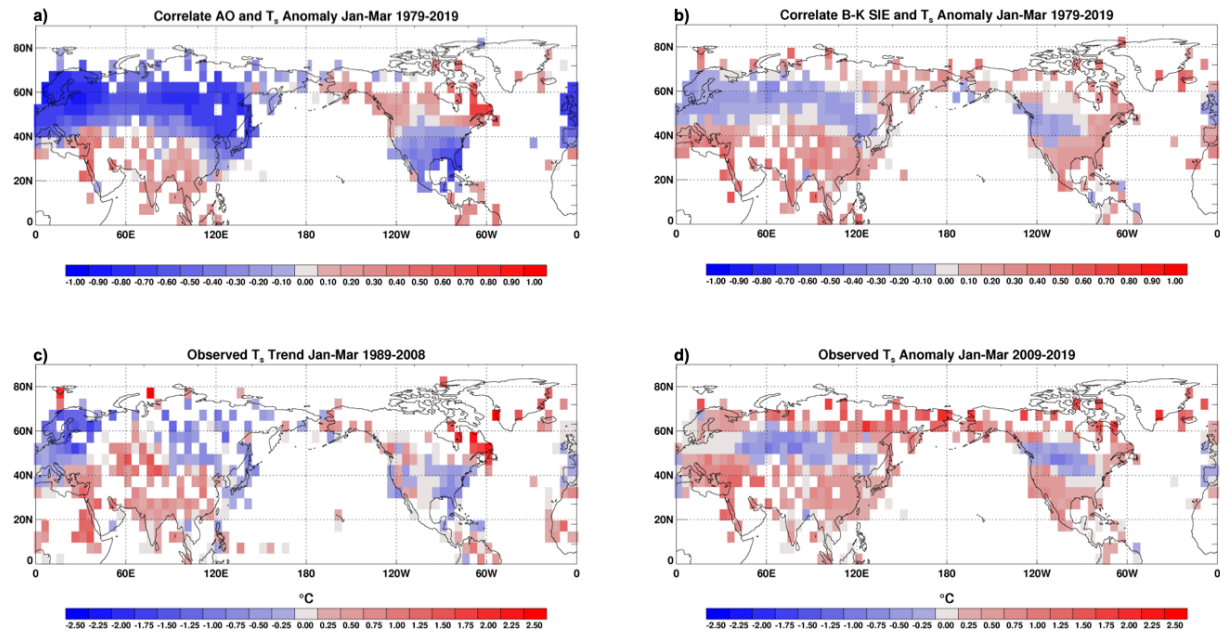
### Winter Mean Surface Temperature Anomalies



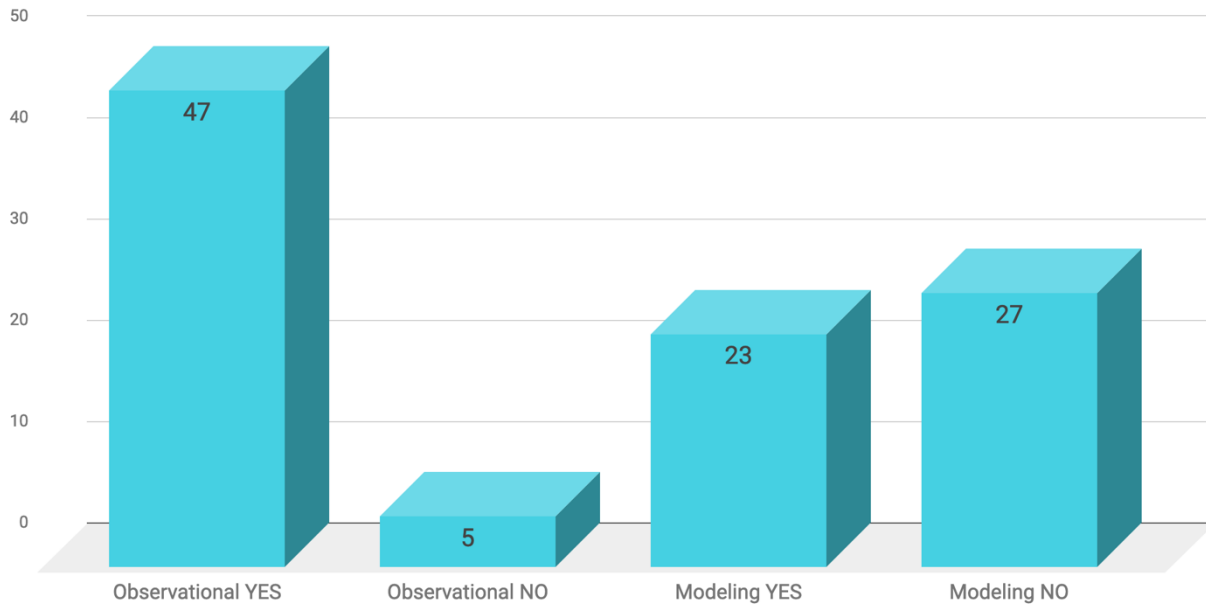
**Supplementary Figure 1. Arctic amplification is increasing.** **a** Mean temperature (averaged for December, January, and February), shown as anomaly from 1951–1980 mean temperatures. The area inside the black box shows the amplified warming in the Arctic. Updated from Wendisch et al.<sup>62</sup> and data are provided by the NASA Goddard Institute for Space Studies. **b** Interannual (solid) and five-year running mean (dashed) of the temperature anomaly time series of December, January and February Arctic (60–90°N; blue), mid-latitude land only (30–60°N; red), and the difference between Arctic and mid-latitude area averaged temperatures (green). Climatology used based on 1981–2010 means. Data is from the NCEP/NCAR reanalysis. Both plots cover data from 1960 through 2019.



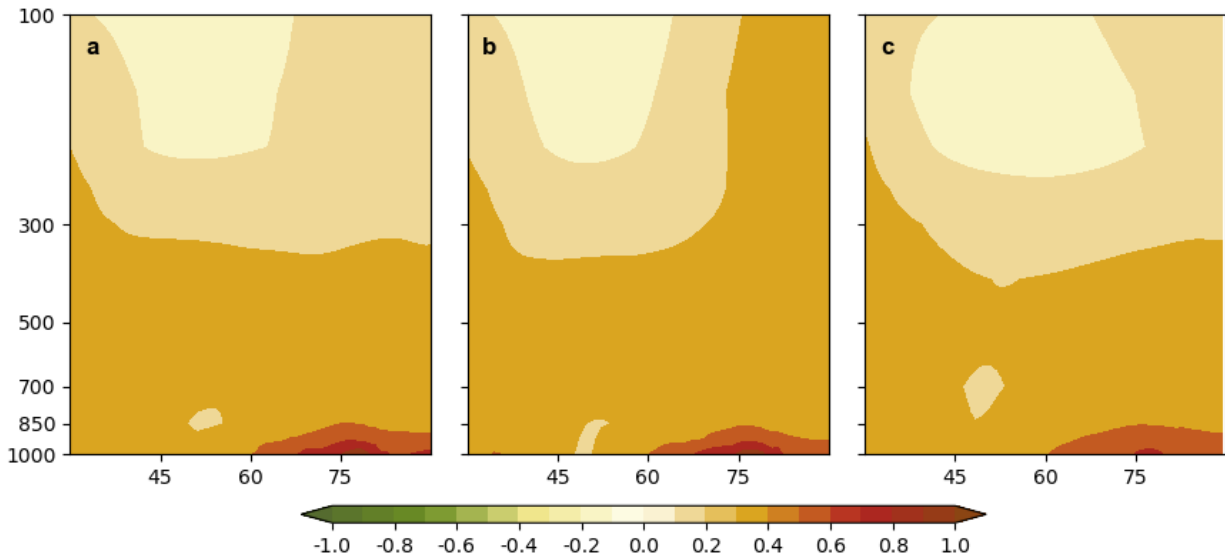
**Supplementary Figure 2. Recent pattern of warming and cooling across NH consistent with earlier trends.** **a** The decadal trend in October, November and December 2-m air temperatures over land surface 1988–2007. **b** The decadal trend in January, February and March 2-m air temperatures over land surface 1989–2008. **c** The average seasonal anomaly for October, November and December 2-m air temperatures over land surface 2008–2018. **d** The average seasonal anomaly for January, February and March 2-m air temperatures over land surface 2009–2019. Colored shading in degrees Celsius; values between  $-0.25$  and  $0.25$  are shown in gray and missing and ocean values are shown in white. Climatology used in all plots are 1981–2010 means. Data is land station data from the Hadley Centre Climate Risk Unit<sup>63</sup>.



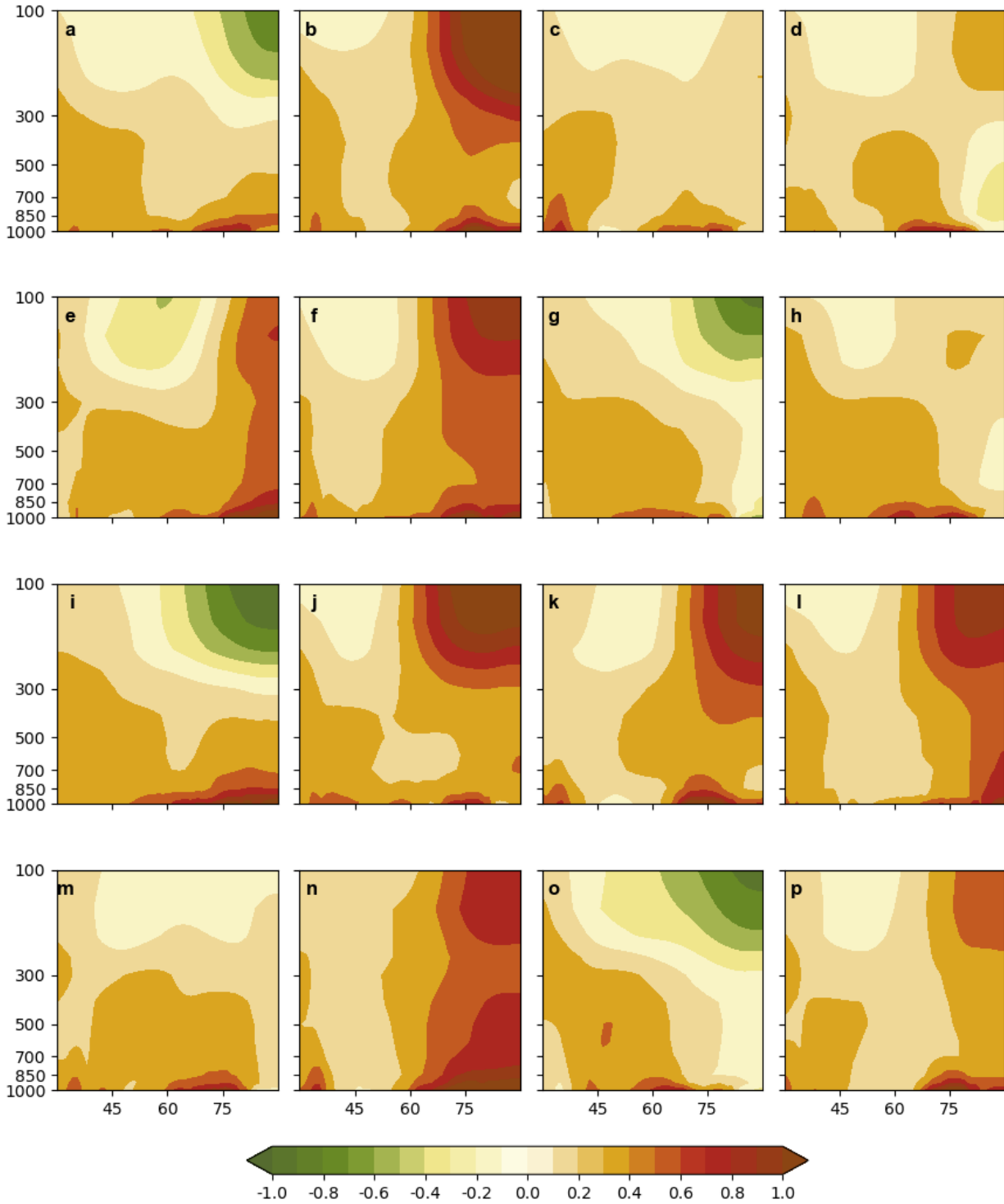
**Supplementary Figure 3. NH temperature is shifting from AO to sea ice pattern of variability.** **a** The correlation between the January, February and March Arctic Oscillation and January, February and March 2-m air temperatures over land surface 1979–2019. **b** The correlation between November Barents-Kara sea ice extent 1978–2018 and January, February and March 2-m air temperatures over land surface 1979–2019. **c** The decadal trend in January, February and March 2-m air temperatures over land surface 1989–2008. **d** The average seasonal anomaly for January, February and March 2-m air temperatures over land surface 2009–2019. Climatology used in all plots are 1981–2010 means. Data is land station data from the Hadley Centre Climate Risk Unit<sup>63</sup>.



**Supplementary Figure 4. Studies arguing for and against a link between AA and an increase in severe winter weather are divided.** Number of observational/modeling studies that support AA is linked with an increase in severe winter weather and observational/modeling studies that support AA is not linked with an increase in severe winter weather. A list of the studies behind the bar graph can be found here: [List of Studies](#).

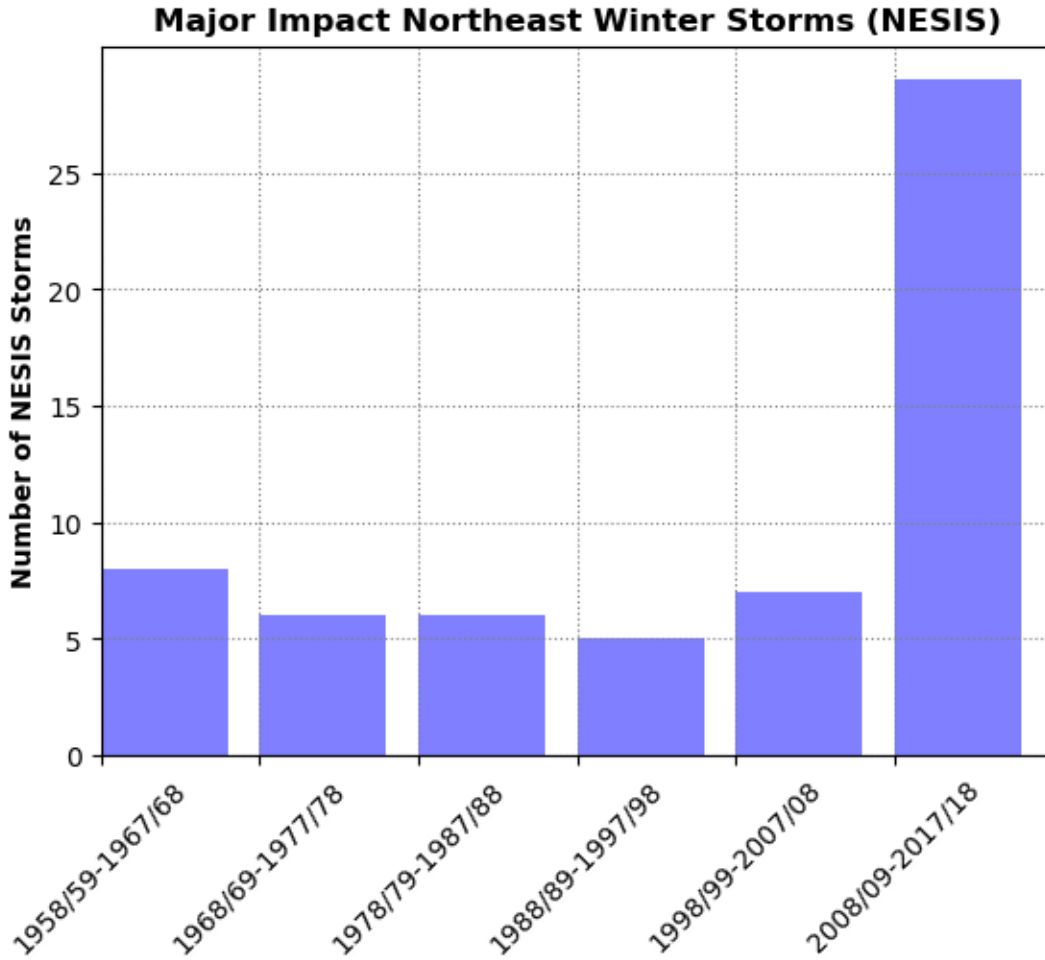


**Supplementary Figure 5. Simulated temperature trends consistent among model experiments.** Seasonal and zonal-mean air temperature trends in degrees Celsius per decade from 1981–2015 for the average of ensemble members for **a** Community Atmosphere Model (low top), **b** Community Atmosphere Model (high top), and **c** ECHAM model.



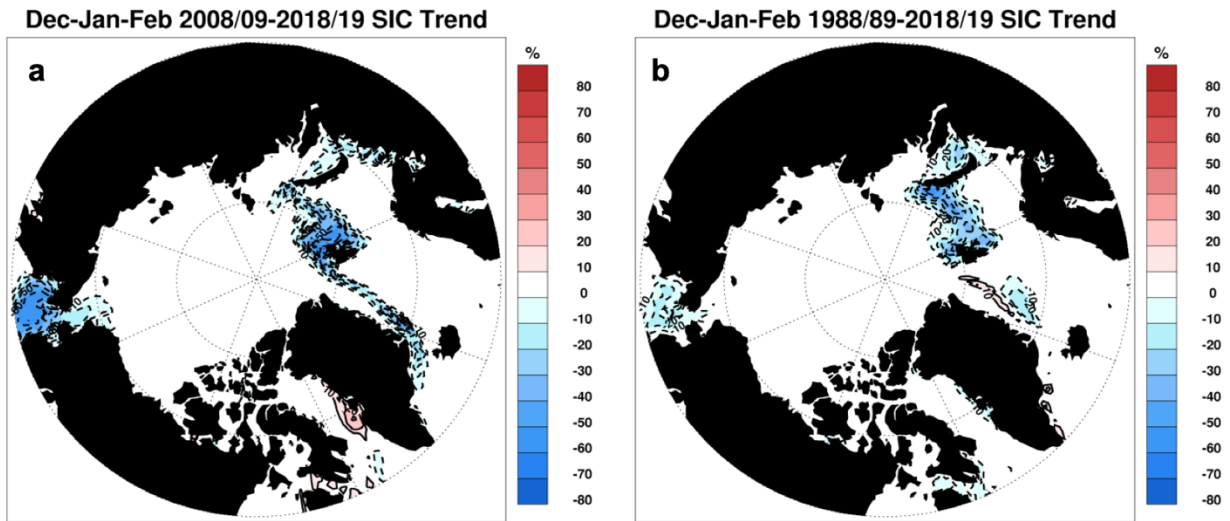
**Supplementary Figure 6. Simulated temperature trends vary greatly among ensemble members.** Seasonal and zonal-mean air temperature trends in degrees Celsius per decade from 1981–2015 for 16 (**a – p**) ensemble members of the Community Atmosphere Model (high top).



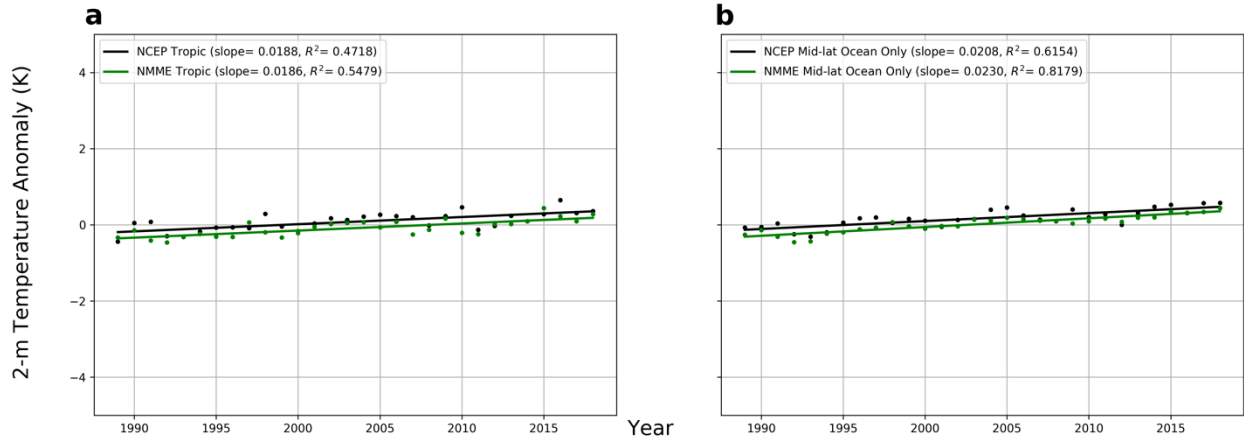


**Supplementary Figure 7. Impactful Northeast US snowstorms tripled over the past decade.**

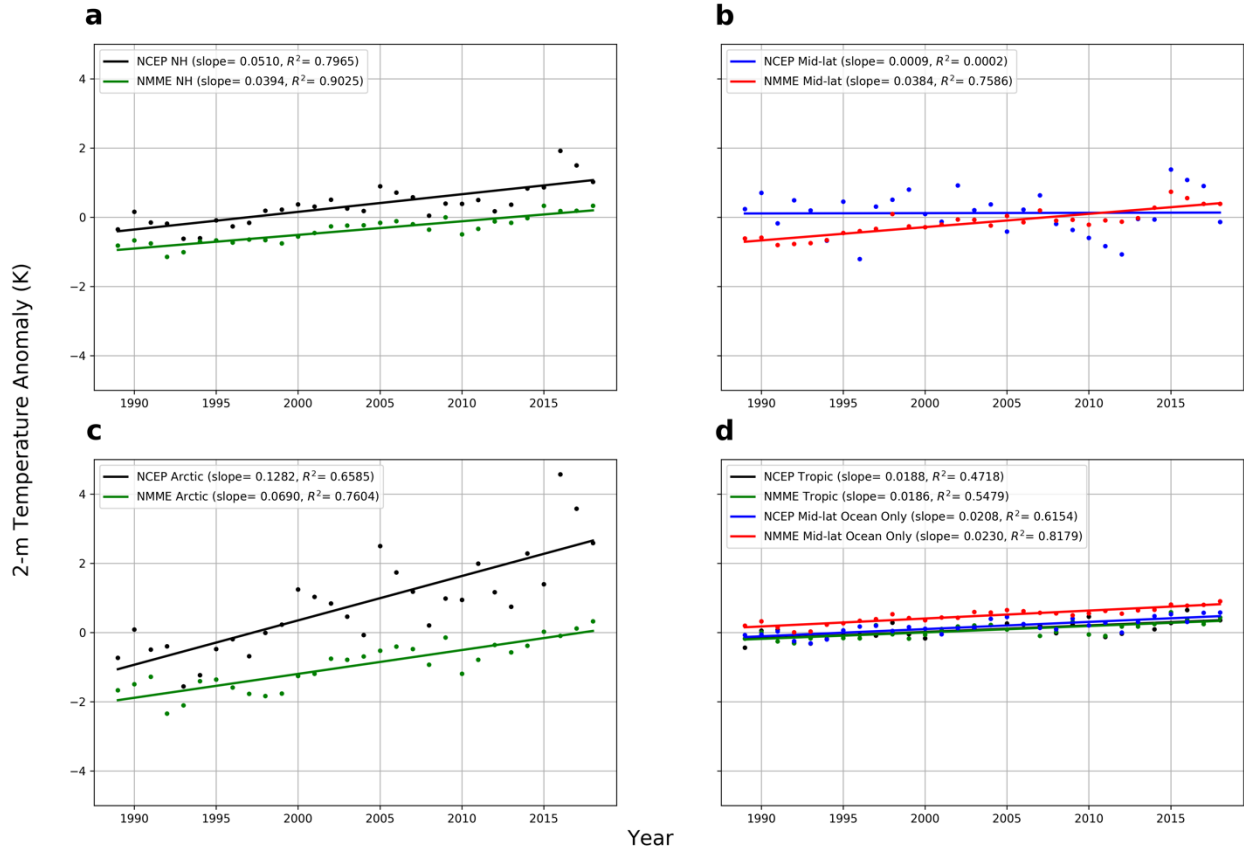
Number of impactful snowstorms in the Northeastern US is triple in number over the most recent decade compared to all previous decades. The number of major impact Northeastern US winter storms referred to as Northeast Snowfall Impact Scale (NESIS) per decade starting from winter 1958/59. Data available from NOAA <https://www.ncdc.noaa.gov/snow-and-ice/rsi/nesis>.



**Supplementary Figure 8. Sea ice loss is greatest in Barents-Kara, Chukchi-Bering Seas and around Greenland. a** Linear decadal-trends in winter Arctic sea ice concentration from 2008/09 through 2017/18 (multiplied by 100). **b** Linear trends in winter Arctic sea ice concentration from 1988/89 through 2017/18 (multiplied by 200).



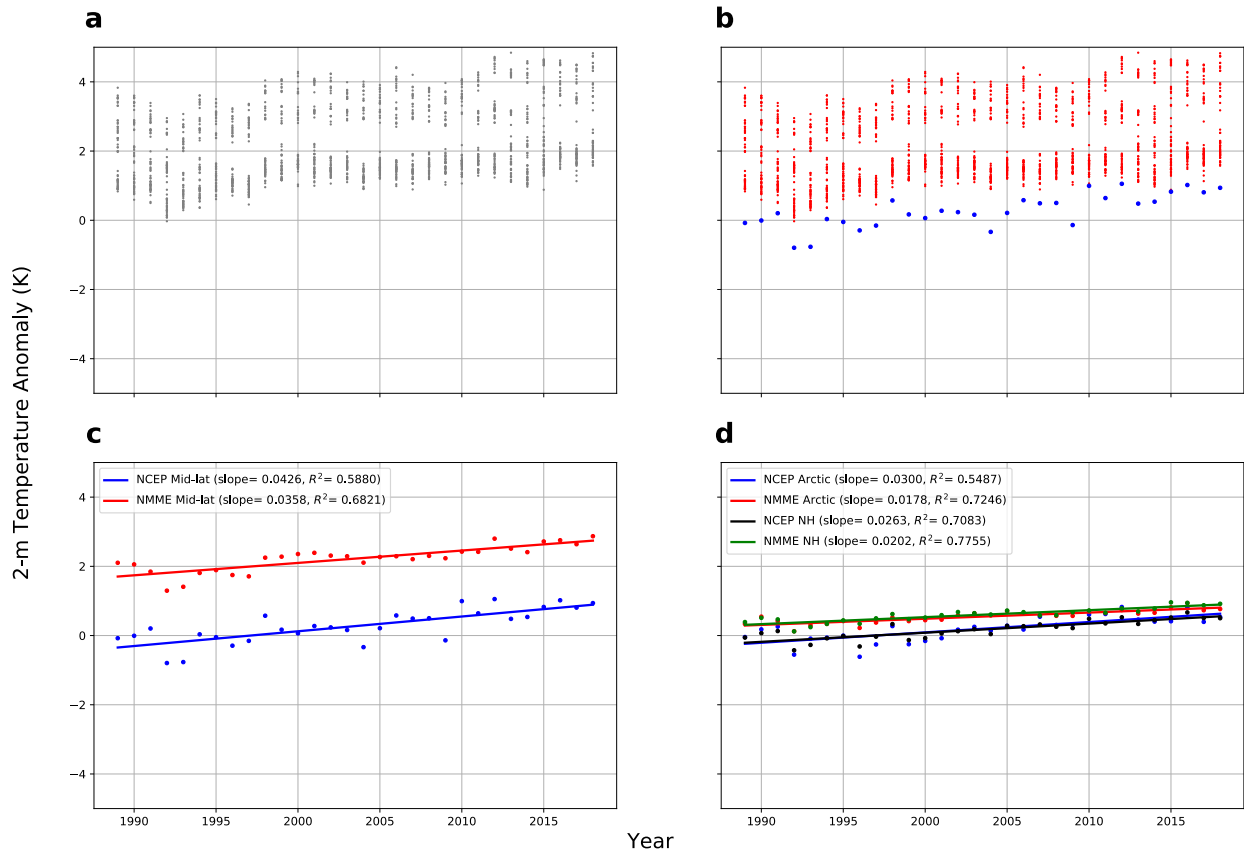
**Supplementary Figure 9. Observed and simulated warming match in the tropics and mid-latitude oceans.** **a** Reanalysis (black) and hindcasted/predicted NMME ensemble mean (green) NH tropical 2-meter temperature anomalies and linear trends. **b** Reanalysis (black) and hindcasted/predicted NH NMME ensemble mean (green) mid-latitude ocean 2-meter temperature anomalies and linear trends. All plots for December, January, February and March from 1988 through 2019 and climatology used for reanalysis is 1981–2010 and for NMME is 1982–2010 winter mean respectively. Variance ( $R^2$ ) included for all trend lines. All trends are statistically significant at the >99% confidence level.



**Supplementary Figure 10. NH warming trends are insensitive to climatology. a** Reanalysis (black) and hindcasted/predicted NMME ensemble mean (green) NH temperature anomalies (black) and linear trends. **b** Reanalysis (blue) and hindcasted/predicted NMME ensemble mean (red) NH continental mid-latitude temperature anomalies and linear trends. **c** Reanalysis (black) and hindcasted/predicted NMME ensemble mean (green) Arctic temperature anomalies and linear trends. **d** Reanalysis (black) and hindcasted/predicted NMME ensemble mean (green) NH tropical 2-meter temperature anomalies and reanalysis (blue) and hindcasted/predicted NH NMME ensemble mean (red) mid-latitude ocean 2-meter temperature anomalies and linear trends. All plots for December, January, February and March from 1988 through 2019 and climatology used is 1981–2010 winter mean from reanalysis only. Variance ( $R^2$ ) included for all trend lines. All

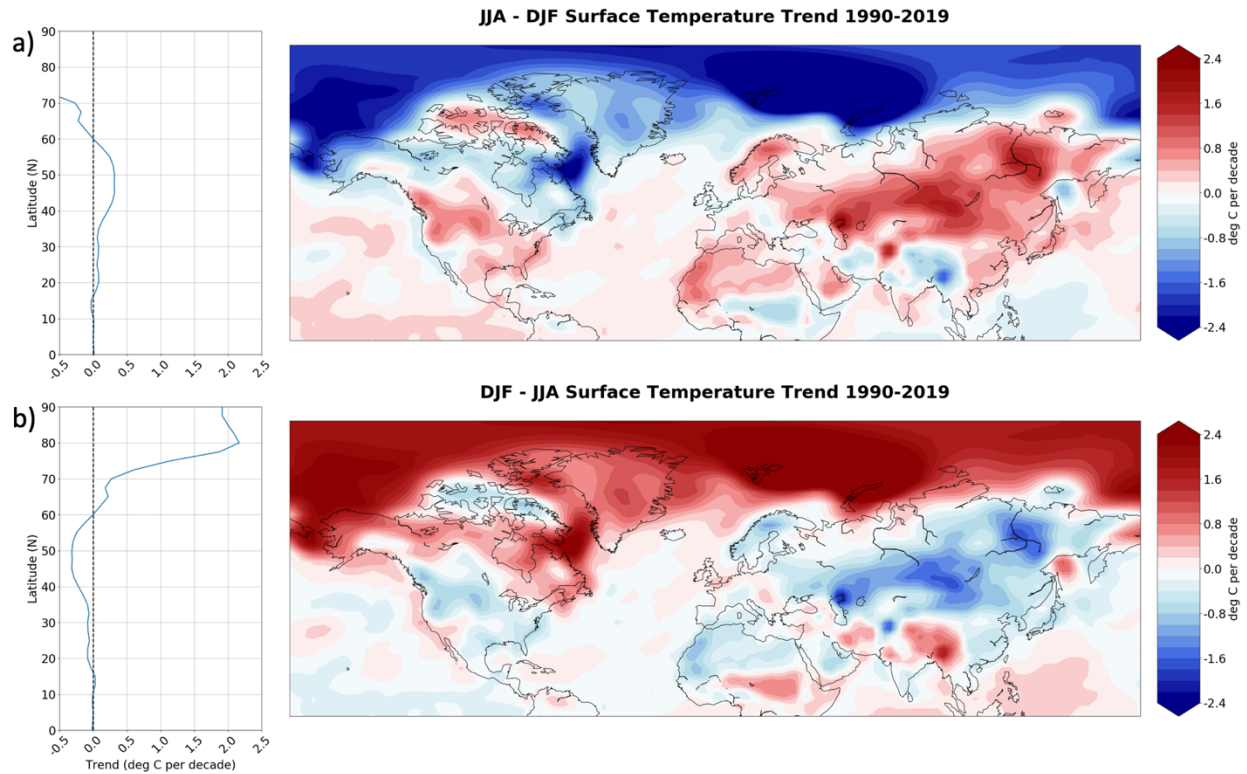
trends except the NCEP mid-latitude land regions are statistically significant at the >99% confidence level.

## JJA analysis



**Supplementary Figure 11. Observed and simulated Arctic and mid-latitude summer temperature trends are parallel. a** Reanalysis and hindcasted/predicted NMME individual ensemble members for NH mid-latitude continental temperature anomalies. **b** Same as **a** but reanalysis (blue) and NMME (red). **c** Reanalysis (blue) and hindcasted/predicted NMME ensemble mean (red) NH mid-latitude continental temperature anomalies. Also included is the linear trend line for each dataset. **d** Reanalysis (black) and hindcasted/predicted NMME ensemble mean (green) NH temperature anomalies and reanalysis (blue) and hindcasted/predicted NMME ensemble mean (red) Arctic temperature anomalies and linear trends. All temperature anomalies are for June, July and August from 1989 through 2018. Anomalies are calculated relative to climatology from reanalysis 1981–2010 and from NMME 1982–2010 summer mean respectively.

Variance ( $R^2$ ) included for all trend lines. All trends except the NCEP NH mid-latitude land regions are statistically significant at the >99% confidence level.



**Supplementary Figure 12. Summer minus winter temperature trends and vice versa are consistent with warm Arctic-cold continents pattern. a** Summer minus winter temperature trends from 1990 through 2019 show a relatively cold Arctic and warm midlatitudes. Temperature trend difference by latitude shown on the right. **b** Same as **a** but for winter minus summer temperature trends. Data taken from NCEP/NCAR reanalysis.



**Supplementary Table 1.** List of coupled climate models from the CMIP5 model archive analyzed in this study.

<b>Institute</b>	<b>model</b>
National Aeronautics and Space Administration (NASA) Goddard Institute for Space Studies (GISS), United States of America	GISS-E2-R-CC
	GISS-E2-R
	GISS-E2-H-CC
EC-EARTH consortium	EC-EARTH
Centre National de Recherches Météorologiques/Centre Européen de Recherche et Formation Avancées en Calcul Scientifique (CNRM-CERFACS), France	CNRM-CM5
National Institute of Meteorological Research/Korea Meteorological Administration	HadGEM2-AO
Max Planck Institute for Meteorology (MPI-M), Germany	MPI-ESM-MR
	MPI-ESM-LR
Beijing Normal University (BNU), China	BNU-ESM
Commonwealth Scientific and Industrial Research Organisation (CSIRO) in collaboration with the Queensland Climate Change Centre of Excellence (QCCCE), Australia	CSIRO-Mk3.6.0
Institut Pierre-Simon Laplace	IPSL-CM5A-LR
	IPSL-CM5B-LR
	IPSL-CM5A-MR
National Center for Atmospheric Research (NCAR), United States	CCSM4
Met Office Hadley Centre (additional HadGEM2-ES realizations contributed by Instituto Nacional de Pesquisas Espaciais)	HadGEM2-ES
	HadGEM2-CC
Institute of Numerical Mathematics (INM), Russia	INM-CM4
Atmosphere and Ocean Research Institute (The University of Tokyo)/National Institute for Environmental Studies/Japan Agency for Marine-Earth Science and Technology, Japan	MIROC5
	MIROC-ESM-CHEM
	MIROC-ESM
National Center for Atmospheric Research (NCAR), United States	CESM1\ (WACCM)
	CESM1\ (CAM5)
	CESM1\ (BGC)
Canadian Centre for Climate Modeling and Analysis (CCCma), Canada	CanESM2
Institute of Atmospheric Physics, Chinese Academy of Sciences	FGOALS-s2
National Oceanic and Atmospheric Administration (NOAA)- Geophysical Fluid Dynamics Laboratory	GFDL-CM3

Norwegian Climate Centre (NCC), Norway	NorESM1-M
	NorESM1-ME
The First Institute of Oceanography, SOA, China	FIO-ESM
Beijing Climate Center (BCC), China	BCC-CSM1.1(m)
	BCC-CSM1.1
CSIRO (Commonwealth Scientific and Industrial Research Organisation, Australia), and BOM (Bureau of Meteorology, Australia)	ACCESS1.3
	ACCESS1.0
Meteorological Research Institute (MRI), Japan	MRI-CGCM3
Centro Euro-Mediterraneo per I Cambiamenti Climatici	CMCC-CM
	CMCC-CMS
	CMCC-CESM
Institute of Atmospheric Physics (IAP) and Tsinghua University, China	FGOALS-g2

## References

1. Cohen, J. *et al.* Recent Arctic amplification and extreme mid-latitude weather. *Nat. Geosci.* **7**, 627–637, <https://doi.org/10.1038/ngeo2234> (2014).
2. Horton, R. *et al.* Contribution of changes in atmospheric circulation patterns to extreme temperature trends. *Nature* **522**, 465–469 <https://doi.org/10.1038/nature14550> (2015).
3. Kwok, R. *et al.* Thinning and volume loss of the Arctic Ocean sea ice cover: 2003–2008. *J. Geophys. Res.* **114**, <https://doi.org/10.1029/2009JC005312> (2009).
4. Lang, A., Yang, S. & Kass, E. Sea ice thickness and recent Arctic warming. *Geophys. Res. Lett.* **44**, 409–418, <https://doi.org/10.1002/2016GL071274> (2017).
5. Stroeve, J. C., Markus, T., Boisvert, L., Miller, J. & Barrett, A. Changes in Arctic melt season and implications for sea ice loss. *Geophys. Res. Lett.* **41**, 1216–1225, <https://doi.org/10.1002/2013GL058951> (2014).
6. Taylor, P. C., Hegyi, B. M., Boeke, R. C. & Boisvert, L. N. On the increasing importance of air-sea exchanges in a thawing Arctic: A review. *Atmos.* **9**, <https://doi.org/10.3390/atmos9020041> (2018).
7. Ding, Q. *et al.* Influence of high-latitude atmospheric circulation changes on summertime Arctic sea ice. *Nat. Clim. Change* **7**, 289–295, <https://doi.org/10.1038/NCLIMATE3241> (2017).
8. Serreze, M. C. & Francis, J. A. The arctic amplification debate. *Climatic Change* **76**(3–4), 241–264, <https://doi.org/1007/s10584-005-9017-y> (2006).
9. Screen, J. A. & Simmonds, I. The central role of diminishing sea ice in recent Arctic temperature amplification. *Nature* **464**, 1334–1337, <https://doi.org/10.1038/nature09051> (2010).

10. Kay, J. E. & L'Ecuyer, T. Observational constraints on Arctic ocean clouds and radiative fluxes during the early 21<sup>st</sup> century. *J. Geophys. Res. Atmos.* **118**, 7219–7236, <https://doi:10.1002/jgrd.50489> (2013).
11. Boeke, R. C. & Taylor, P. C. Seasonal energy exchange in sea ice retreat regions contributes to differences in projected Arctic warming. *Nature Comm.* **9**, 5017, <https://doi:10.1038/s41467-018-07061-9> (2018).
12. Uttal, T. *et al.* Surface heat budget of the Arctic Ocean. *Bull. Amer. Meteor. Soc.* **83**, 255–275, [https://doi:10.1175/1520-0477\(2002\)083<0255:SHBOTA>2.3.CO;2](https://doi:10.1175/1520-0477(2002)083<0255:SHBOTA>2.3.CO;2) (2002).
13. Francis, J. A., Hunter, E., Key, J. R. & Wang, X. Clues to variability in Arctic minimum sea ice extent. *Geophys. Res. Lett.* **32**, <https://doi:10.1029/2005GL024376> (2005).
14. Screen, J. A. Simulated atmospheric response to regional and Pan-Arctic sea-ice loss. *J. Climate* **30**, <https://doi.org/10.1175/JCLI-D-16-0197.1> (2017).
15. Liu, Y. & Key, J. R. Assessment of Arctic cloud cover anomalies in atmospheric reanalysis products using satellite data. *J. Climate* **29**, 6065–6083, <https://doi:10.1175/JCLI-D-15-0861.1> (2016).
16. Lee, S. A theory for polar amplification from a general circulation perspective. *Asia-Pac. J. Atmos. Sci.* **50**, 31–43, <https://doi.org/10.1007/s13143-014-0024-7> (2014).
17. Park, H.-S., Lee, S., Son, S.-W., Feldstein, S. B. & Kosaka, Y. The impact of poleward moisture and sensible heat flux on Arctic winter sea-ice variability. *J. Climate* **28**, 5030–5040, <https://doi:10.1175/JCLI-D-15-0074.1> (2015).

18. Cohen, J., *et al.* Arctic change and possible influence on mid-latitude climate and weather. US CLIVAR Report 2018-1, 41pp, <https://doi:10.5065/D6TH8KGW> (2018).
19. Doyle, J. G., *et al.* Water vapor intrusions into the high Arctic during winter. *Geophys. Res. Lett.* **38**, <https://doi:10.1029/2011GL047493> (2011).
20. Kapsch, M.-L., Graversen, R. G., Tjernström, M. & Bintanja, R. The effect of downwelling longwave and shortwave radiation on Arctic summer sea ice. *J. Climate* **29**, 1143–1159, <https://doi:10.1175/JCLI-D-15-0238.1> (2016).
21. Hegyi, B. M. & Taylor, P. C. The unprecedented 2016-17 Arctic sea ice growth season: The crucial role of atmospheric rivers and longwave fluxes. *Geophys. Res. Lett.* **45**, 5204–5212, <https://doi.org/10.1029/2017GL076717> (2018).
22. Kapcsch, M.-L., Graversen R. G. & Tjernstrom, M. Springtime atmospheric energy transport and the control of Arctic summer sea-ice extent. *Nature Climate Change*, **3**, 744–748 <https://doi:10.1038/nclimate1884> (2013).
23. Yang, W. & Magnusdottir, G. Springtime extreme moisture transport into the Arctic and its impact on sea ice concentration. *J. Geophys. Res. Atmos.* **122**, 5516–5329, <https://doi:10.1002/2016JD026324> (2017).
24. Yang, W. & Magnusdottir, G. Year-to-year variability in Arctic minimum sea ice extent and its preconditions in observations and the CESM Large Ensemble simulations. *Scientific Reports*, <https://doi.org/10.1038/s41598-018-27149-y> (2018).

25. Lee, S., Gong, T. T., Johnson, N. C., Feldstein, S. B. & Pollard, D. On the possible link between tropical convection and the Northern Hemisphere Arctic surface air temperature change between 1958-2001. *J. Climate* **24**, 4350–4367, <https://doi.org/10.1175/2011JCLI4003.1> (2011).
26. Cvijanovic, I. *et al.* Future loss of Arctic sea-ice cover could drive a substantial decrease in California’s rainfall. *Nat. Comm.*, <https://doi.org/10.1038/s41467-017-01907-4> (2017).
27. Lee, S. Testing of the tropically excited Arctic warming (TEAM) mechanism with traditional El Niño and La Niña. *J. Climate* **25**, 4015–4022, <https://doi.org/10.1175/JCLI-D-12-00055.1> (2012).
28. Yoo, C., Lee, S. & Feldstein, A. Arctic response to an MJO-like tropical heating in an idealized GCM. *J. Atmos. Sci.* **69**, 2379–2393, <https://doi.org/10.1175/JAS-D-11-0261.1> (2012a).
29. Yoo, C., Lee, S. & Feldstein, S. B. Mechanisms of Arctic surface air temperature change in response to the Madden-Julian Oscillation. *J. Climate* **25**, 5777–5790, <https://doi.org/10.1175/JCLI-D-11-00566.1> (2012b).
30. Henderson, G. R., Barrett, B. S. & LaFleur, D. M. Arctic sea ice and the Madden-Julian Oscillation (MJO). *Climate Dyn.* **43**, 2185–2196, <https://doi.org/10.1007/s00382-013-2043-y> (2014).
31. Goss, M., Feldstein, S. B. & Lee, S. Stationary wave interference, and its relation to tropical convection and Arctic warming. *J. Climate* **29**, 1369–1389, <https://doi.org/10.1175/JCLI-D-15-0267.1> (2016).
32. Honda, M., Inoue, J. & Yamane, S. Influence of low Arctic sea-ice minima on anomalously cold Eurasian winters. *Geophys. Res. Lett.* **36**, <https://doi.org/10.1029/2008GL037079> (2009).

33. Orsolini, Y., Senan, R., Benestad, R. E. & Melsom, A. Autumn atmospheric response to the 2007 low Arctic sea ice extent in coupled ocean-atmosphere hindcasts. *Climate Dyn.* **38**, 2437–2448, <https://doi.org/10.1007/s00382-011-1169-z> (2012).
34. Wegmann, M. *et al.* Arctic moisture source for Eurasian snow cover variations in autumn. *Environ. Res. Lett.* **10**, <https://doi.org/10.1088/1748-9326/10/5/054015> (2015).
35. Cohen, J., Furtado, J., Jones, J., Barlow, M., Whittleston, D. & Entekhabi, D. Linking Siberian snow cover to precursors of stratospheric variability. *J. Climate* **27**, 5422–5432 (2014).
36. Overland, J. E. *et al.* The melting Arctic and mid-latitude weather patterns: Are they connected? *J. Climate* **28**, 7917–7932, <https://doi.org/10.1175/JCLI-D-14-00822.1> (2015).
37. Zuo, J., Ren, H. L., Wu, B. & Li, W. Predictability of winter temperature in China from previous autumn Arctic sea ice. *Climate Dyn.* **47**, 2331, <https://doi.org/10.1007/s00382-015-2966-6> (2016).
38. Overland, J. E. & Wang, M. Arctic-midlatitude weather linkages in North America. *Polar Sci.* **16**, 1–9, <https://doi.org/10.1016/j.polar.2018.02.001> (2018).
39. Kug, J.-S. *et al.* Two distinct influences of Arctic warming on cold winters over North America and East Asia. *Nat. Geosci.* **8**, 759–762, <https://doi.org/10.1038/ngeo2517> (2015).
40. Lee, M.-Y., Hong, C.-C. & Hsu, H.-H. Compounding effects of warm sea surface temperature and reduced sea ice on the extreme circulation over the extratropical North Pacific and North America during the 2013–2014 boreal winter. *Geophys. Res. Lett.* **42**, 1612–1618, <https://doi.org/10.1002/2014GL062956> (2015).

41. Cohen, J. An observational analysis: Tropical relative to Arctic influence on midlatitude weather in the era of Arctic amplification. *Geophys. Res. Lett.* **43**, 5287–5294, <https://doi.org/10.1002/2016GL069102> (2016).
42. Baxter, S. & Nigam, S. Key role of North Pacific oscillation/West Pacific pattern in generating the extreme 2013–2014 North American winter. *J. Climate* **28**, 8109–8117, <https://doi.org/10.1175/JCLI-D-14-00726.1> (2015).
43. Ding, Q. *et al.* Tropical forcing of the recent rapid Arctic warming in northeastern Canada and Greenland. *Nature* **509**, 209–212, <https://doi.org/10.1038/nature13260> (2014).
44. Sun, L., Perlwitz, J. & Hoerling, M. What caused the recent “Warm Arctic, Cold Continents” trend pattern in winter temperatures? *Geophys. Res. Lett.* **43**, 5345–5352 (2016).
45. Ballinger, T. *et al.* Greenland coastal air temperatures linked to Baffin Bay and Greenland Sea ice conditions during autumn through regional blocking patterns. *Climate Dyn.* **50**, 83–100, <https://doi.org/10.1007/s00382-017-3583-3> (2018).
46. Chen, X. & Luo, D. Arctic sea ice decline and continental cold anomalies: Upstream and downstream effects of Greenland blocking. *Geophys. Res. Lett.* **44**, 3411–3419, <https://doi.org/10.1002/2016GL072387> (2017).
47. Woollings, T., Hannachi, A. & Hoskins, B. Variability of the North Atlantic eddy-driven jet stream. *Quart. J. Roy. Meteor. Soc.* **136**, 856–868, <https://doi.org/10.1002/qj.625> (2010).
48. Petoukhov, V. & Semenov, V. A link between reduced Barents-Kara sea ice and cold winter extremes over northern continents. *J. Geophys. Res.* **115**, <https://doi.org/10.1029/2009JD013568> (2010).



49. Liptak, J. & Strong, C. The winter atmospheric response to sea ice anomalies in the Barents Sea. *J. Climate* **27**, 914–924, <https://doi.org/10.1175/JCLI-D-13-00186.1> (2014).
50. Sun, L., Deser, C. & Tomas, R. A. Mechanisms of stratospheric and tropospheric circulation response to projected Arctic sea ice loss. *J. Climate* **28**, 7824–7845, <https://doi.org/10.1175/JCLI-D-15-0169.1> (2015).
51. Peings, Y. & Magnusdottir, G. Response of the wintertime Northern Hemisphere atmospheric circulation to current and projected Arctic sea ice decline: A numerical study with CAM5. *J. Climate* **27**, 244–264, <https://doi.org/10.1175/JCLI-D-13-00272.1> (2014).
52. Semenov V. A. & Latif, M. Nonlinear winter atmospheric circulation response to Arctic sea ice concentration anomalies for different periods during 1966–2012. *Environ. Res. Lett.* **10**(5), 054020, <https://doi.org/10.1088/1748-9326/10/5/054020> (2015).
53. Chen, H. W., Zhang, F. & Alley, R. B. The robustness of midlatitude weather pattern changes due to Arctic sea ice loss. *J. Climate* **29**, 7831–7849, <https://doi.org/10.1175/JCLI-D-16-0167.1> (2016).
54. Overland, J. E., Francis, J. A., Hanna, E. & Wang, M. The recent shift in early summer Arctic atmospheric circulation. *Geophys. Res. Lett.* **39**, L19804, <https://doi.org/10.1029/2012GL053268> (2012).
55. Coumou, D., Petoukhov, V., Rahmstorf, S., Petri, S. & Schellnhuber, H. J. Quasi-resonant circulation regimes and hemispheric synchronization of extreme weather in boreal summer. *Proc. Nat. Acad. Sci.* **111**, 12331–12336, <https://doi.org/10.1073/pnas.1412797111> (2014).

56. Coumou, D., Lehmann, J. & Beckmann, J. The weakening summer circulation in the Northern Hemisphere mid-latitudes. *Science* **348**, 324–327, <https://doi.org/10.1126/science.1261768> (2015).
57. Lehmann, J., Coumou, D., Frieler, K., Eliseev, A. V. & Levermann, A. Future changes in extratropical storm tracks and baroclinicity under climate change. *Environ. Res. Lett.* **9**, <https://doi.org/10.1088/1748-9326/9/8/084002> (2014).
58. Chang, E. K. M., Ma, C.-G., Zheng, C. & Yau, A. M. W. Observed and projected decrease in Northern Hemisphere extratropical cyclone activity in summer and its impacts on maximum temperature. *Geophys. Res. Lett.* **43**, 2200–2208, <https://doi:10.1002/2016GL068172> (2016).
59. Coumou, D., Kornhuber, K., Lehmann, J. & Petoukhov, V. Weakened flow, persistent circulation, and prolonged weather extremes in boreal summer. *Climate Extremes: Patterns and Mechanisms*, *Geophys. Monogr.* 226, S.-Y. Wang, J.-H. Yoon, C. C. Funk, and R. R. Gilles, Eds., Amer. Geophys. Union, 61–74, ISBN:978119067849 (2017).
60. Coumou, D., Di Capua, G., Vavrus, S., Wang, L. & Wang, S. The influence of Arctic Amplification on mid-latitude summer circulation. *Nat. Comm.* (2018 in revision).
61. Blackport, R., Screen, J. A., van der Wiel, K. & Bintanja, R. Minimal influence of reduced Arctic sea ice on coincident cold winters in mid-latitudes. *Nature Climate Change* **9**, 697–704, <https://doi.org/10.1038/s41558-019-0551-4> (2019).
62. Wendisch, M. *et al.* Understanding causes and effects of rapid warming in the Arctic. *Eos* **98**, <https://doi.org/10.1029/2017EO064803> (2017).

63. Morice, C. P., Kennedy, J. J., Rayner, N. A. & Jones, P. D. Quantifying uncertainties in global and regional temperature change using an ensemble of observational estimates: the HadCRUT4 dataset. *J. Geophys. Res.* **117**, D08101, <https://doi:10.1029/2011JD017187> (2012).